J Electroceram (2010) 25:60–69
DOI 10.1007/s10832-009-9589-4

Impedance spectroscopy studies of $K_{0.5}Bi_{0.5}TiO_3$

P. Vijaya Bhaskar Rao · T. Bhima Sankaram

Received: 12 May 2006 / Accepted: 31 August 2009 / Published online: 2 October 2009

Abstract Lead free Potassium bismuth Titanate $K_{0.5}Bi_{0.5}TiO_3$ (KBT) was prepared by high temperature solid state reaction method in a closed crucible with excess KBT powder around the samples. A room temperature study of XRD confirms, single phase formation with tetragonal structure .Grain and grain boundary conduction is observed from complex impedance spectrum at high temperatures (425°C) by the appearance of two semicircular arcs. The Cole-Cole plots of impedance spectrum consisted of a Circular arc followed by a semicircular spur indicate that the dielectric phenomenon of KBT is due to conductive grain boundaries. The temperature variation of grain resistance and grain boundary resistance is observed with the activation energies. The presence of non-Debye type multiple relaxations has been confirmed by complex modulus analysis. The dielectric data obtained from impedance measurements, indicates broad dielectric peaks around 380°C. The ferroelectric nature confirmed from hysteresis plot. The DC Conductivity results indicate activation energy 0.54 eV below 400°C and 0.85 eV above 400°C. The AC conductivity values and electric modulus values are computed from the impedance data. The activation energies of AC conductivity have observed to decrease with decrease in frequencies.

Keywords $K_{0.5}Bi_{0.5}TiO_3$ · Impedance spectroscopy · Cole-Cole polts · Dielectric relaxation · Conductivity

P. V. B. Rao (✉)
Department of Physics, CVR College of Engineering,
Vasthu Nagar, Mangalpally, RR district-501510,
Andhra Pradesh, India
e-mail: poluri_vijay@rediffmail.com

T. B. Sankaram
Materials Research Laboratory, Department of Physics,
Osmania University,
Hyderabad 500007, Andhra Pradesh, India

1 Introduction

Potassium bismuth titanate, $K_{0.5}Bi_{0.5}TiO_3$ (KBT) and sodium bismuth titanate, $Na_{0.5}Bi_{0.5}TiO_3$ (NBT) belong to the category of perovskites, composed of $A_{0.5}^{+}$ $Bi_{0.5}^{3+}$ B^{4+} O_3, which are receiving greater attention [1–3]. NBT exhibits two structural phase transitions from ferroelectric rhombohedral to tetragonal (~200–350°C) and to para-electric high temperature cubic phase (520–540°C) [4–8]. At about 320°C, NBT exhibits a broad maximum of electric permittivity. NBT-based multi-component solid solution systems have been widely studied [9, 10]. But, compared to NBT, KBT is a much less studied material, because it is difficult to prepare a dense ceramic body by a conventional ceramic fabrication process.

KBT, first discovered by Smolenskii et al. [11], and has a perovskite-type ferroelectric structure belonging to tetragonal crystal system at room temperature. It undergoes a phase transition around 380°C, the ferroelectric Curie point. Ivanova et al. [12] investigated the crystal structure of KBT ceramics by X-ray diffraction analysis, and they reported that the lattice constants of KBT ceramics are a=0.3913 nm, c= 0.3993 nm .They also reported that the second-phase transition temperature T_2, that is, from tetragonal to pseudo cubic, existed at about 270°C. However, the electrical behavior at T_2 has not been investigated. Gadzieve et al. [13] observed this second order phase transition at 300°C and they ascribe this phase transition as the one associated with anti-ferroelectric character of the phase. However, NBT has a T_2 of about 200°C, the same as that of KBT. That is, the phase boundary between the rhombohedral ferroelectric and anti-ferroelectric phase fields and piezo-electricity disappear at T_2.

Li et al. [14] reported the dielectric relaxor properties of ferroelectric $K_{0.5}Bi_{0.5}TiO_3$ prepared by sol-gel method.

Their structural studies indicate the tetragonal lattice type for KBT with point group 4 mm and lattice parameters a=3.941A° and c=4.000A°. However, their compound also contains very small quantities of $K_4Ti_3O_8$ impurity. This particular impurity phase gives extra peak at diffractive angles 15.14° and 16.48°.These two peaks are caused by slight volatization of Bi during sintering. They suggested that, a more detail work should be done on KBT, both from the experimental and theoretical point of view.

Zaremba [15] reported the application of thermal X-ray phase analysis and DTA-TG Curves on KBT. According to the report, KBT can be formed only through the intermediate binary compounds, bismuth titanate ($Bi_2Ti_2O_7$) and potassium titanate rich in TiO_2. Emel'yanova et al. [16] reported the T_C of KBT at 377°C. Under a strong D.C electric field applied to ceramic sample, a shift in T_C towards higher temperature and a decrease in dielectric constant were observed. KBT exhibits hysteresis loop up to 320°C and a pyroelectric maximum at 377°C, indicating the ferroelectric nature [17]. The samples exhibit a spontaneous polarization of 0.68 μC/cm^2 with E_C=50–60 KV/cm. Yang et al. [18], from the ferroelectric properties of KBT thin films prepared on p-type Si (111) substrate suggest that the material is a promising one for application in FRAMs. Hiruma et al. [19] report the ferroelectric and piezoelectric properties of hot pressed KBT ceramics. Their structural studies indicate X-ray density of 93% and impurity peaks such as $K_2Ti_6O_{13}$ in ordinary firing method. These peaks gradually increased in the sintering temperature range from 1040°C to 1060°C and above this temperature the sample was melted .The resistivety was low being of the order 10^{11} Ω.cm and it is due to impurity phase. These results clearly reveal that, it is difficult to fabricate dense KBT ceramics with single-phase perovskite structure by ordinary firing method with out using a chemical process. Hence for fabrication of KBT, hot pressed method is superior to ordinary firing method. The reasons being, it is easy to fabricate dense ceramics higher than 97% at lower sintering temperatures, report the resistivety in the order of 10^{13} Ω. cm at room temperature and Curie temperatures 437°C, 410°C at 1 MHz for hot pressed method KBT samples, prepared at 1060°C and 1080°C respectively. They also report the remnant polarization P_r=22.2 μC/cm^2 and coercive field E_C=52.5 kV/cm electromechanical factor K_{33}=0.28 and d_{33}=69.8pC/N for hot pressed method KBT prepared at 1080°C.

The electrical conductivity, grain resistance and grain boundary resistance studies have not been done on these samples, so far by any earlier worker. The CIS is a powerful technique to characterize many electrical properties of materials. It is useful to evaluate and separate the contribution of the overall electrical properties in the frequency domain due to electrode reactions at the electrode/sample interface and migration of ions through the grains and across the grain boundaries in a polycrystalline material.

The goal of impedance measurement is to compute ac electrical conductivity, dielectric constant and observe the frequency explicit behavior of real and imaginary component of impedance. Hence the authors have felt that, impedance studies on KBT would be highly useful because of its role in the lead free piezoelectric materials.

The present authors have undertaken preparation, and characterization of KBT through XRD, Dielectric, hysteresis, d_{33} and impedance analysis.

2 Experimental procedure

$K_{0.5}Bi_{0.5}TiO_3$ ceramic samples were prepared by conventional solid-state double sintering technique. High purity chemicals of K_2CO_3, Bi_2O_3, and TiO_2 were used as the raw materials. Materials, first dried to eliminate any moisture present and then weighed as per the stoichiometry. These powders were mixed thoroughly and ground to obtain fine powders. The powder was uniaxially pressed into a pellet of diameter 2.6 cm and calcined at 850°C for 2 h, keeping in a closed crucible. After first sintering, this pellet was again crushed into fine powder and pressed into cylindrical pellets of convenient size at a pressure of 3 M Pa–4 M Pa. The pressed pellets were finally sintered at temperature 1000°C for 2 h in an alumina lid enclosed crucible, in presence of pre-sintered KBT powder over the samples. The above precaution was taken to take care of any possible loss of potassium and bismuth in the sintered samples [20].

The single-phase formation of the final sintered samples was tested using the Panalytic X-ray Diffractometer (Expert) by CuKα radiation (λ=1.54 A°), at a scanning speed of 2°/min. Silver paste was used for electroding the final sintered samples for measuring impedance values, hysteresis loop and d_{33} values.

Poling of ferroelectric samples is done to align the ferroelectric domains .Ferroelectric ceramics in general, have zero remnant polarization due to the random distribution of the dipoles in different domains. However, these materials can exhibit permanent dipole moment, a strong piezoelectric and pyroelectric response, by the application of DC electric field, usually for a period of time in the temperatures between RT to T_C. This process is referred to as poling at which a single domain state is said to be achieved [21]. The poling becomes effective at temperature higher than room temperature at which they are not highly conducting and can be poled under sufficiently high electric fields. Because of low dielectric strength of air, oil baths or some dielectric equivalent are used in a poling process. The poling of piezoelectric ceramic after fabrication is an

important stage in the manufacture of transducers and has received considerable attention(1) Because of the possibility of dielectric breakdown under high applied fields, the objective in all poling situations is to induce the maximum degree of domain reorientation for the lowest applied field and in the shortest possible time.

It is well known (2) that the poling process occurs by the reversal of 180° domains and the rotation of 90° domains, with a relatively small fraction of domains actually remaining in an altered configuration upon removal of the applied filed.

Electrical poling of the sample was done at 30 kV/cm in a silicon oil bath at a temperature, 150°C, for 30 min. The sample was cooled to room temperature in the presence of the field. The hysteresis measurements were taken on electrically poled samples at room temperature. The loops were traced and the P_r and E_C values for the ceramic were recorded using PE loop tracer system designed by Marine India ltd. The d_{33} coefficient of the poled sample was measured at 100 Hz using a d_{33} meter (Piezotest, PM-100).

The resistance of the sample was measured on unpoled sample by using 61°C Keithley electrometer connected to a PC, with increasing temperature from room temperature up to 600°C. The DC Conductivity of the sample was calculated from the geometrical factors. The resistivity and there by the conductivity (σ) is computed using the formula

$$\sigma = (t/R^*A)$$

Where σ is DC conductivity, R is the resistance of the sample, A the area of the sample and t the thickness of the sample. The experimental data are plotted between log (σ) and inverse temperature (1000/T). These plots are called Arrhenius plots of conductivity.

2.1 Impedance measurements

The CIS is a non-destructive experimental technique for the characterization of micro structural and electrical properties of some electronic materials [12]. The technique is based on analyzing the ac response of a system to a sinusoidal perturbation and subsequent calculation of impedance as a function of the frequency of the perturbation. The analysis of the electrical properties (conductivity, dielectric constant/loss, etc.) carried out using relaxation frequency (v_{max}) values gives unambiguous results when compared with those obtained at arbitrarily selected fixed frequencies. The frequency dependent properties of a material can be described as complex permittivity (ε*), complex impedance (Z*), complex admittance (Y*), complex electric modulus (M*) and dielectric loss or dissipation factor (tan δ). The real (ε′, Z′, Y′, M′) and imaginary (ε″, Z″, Y″, M″) parts of the complex parameters are in turn related to one another as follows:

$$\varepsilon^* = \varepsilon' - j\varepsilon'' \text{ as :}$$

$$\varepsilon' = -\frac{Z''}{\omega C_0(Z'^2+Z''^2)}$$

$$\varepsilon'' = -\frac{Z'}{\omega C_0(Z'^2+Z''^2)}$$

$$M^* = M' + jM'' = \frac{1}{\varepsilon^*} = j\omega\varepsilon_0 Z^*$$

$$Z^* = Z' - jZ'' = \frac{1}{jC_0\varepsilon^*\omega}$$

$$Y^* = Y' + jY'' = j\omega C_0\varepsilon^*$$

$$\tan\delta = \frac{\varepsilon''}{\varepsilon'} = \frac{M''}{M'} = \frac{Z'}{Z''} = \frac{Z'}{Z''}$$

Where $\omega=2\pi f$ is the angular frequency, C_0 is the geometrical capacitance, $j=\sqrt{-1}$ these relations offer wide scope for a graphical analysis of the various parameters under different conditions of temperature or frequency. The useful separation of intergranular phenomena depends ultimately on the choice of an appropriate equivalent circuit to represent the sample properties.

Complex impedance data on KBT samples was recorded using the AUTOLAB impedance analyzer interfaced to a PC in the temperature range of room temperature to 600°C, in the frequency of 100 Hz–1 MHz.

From the impedance, the real part of AC conductivity was calculated as a function of frequency at selected temperatures, using a relation $\sigma'_{a.c.}=Y'^*(t/A)$, where Y′ is the real part of admittance, t and A are the thickness and area of the samples respectively.

3 Results

Phase formation of the KBT samples was confirmed from the X-ray diffractogram (Fig. 1). The diffractogram was indexed as per the standard KBT data and lattice parameters were determined (a=3.93 Å, c=4.02 Å). The values obtained nearly agree with the values obtained by Ivanova et al. [12]. The X-ray diffraction results show that, there is an extra peak located at the diffractive angle of 15.14°. This may be due to the presence of very small quantities of K_4TiO_8 in the compound (JCPDS file NO.41-0167). This particular impurity phase gives an extra peak at diffractive angle 15.14°. This peak is caused by the slight volatization of Bi during the sintering process.

Li et al. [14] in their study of the dielectric relaxor properties of $K_{0.5}Bi_{0.5}TiO_3$ ferroelectrics prepared by sol-gel method reported that the compound contained a very small quantity of $K_4Ti_3O_8$.They also confirm that the impurity

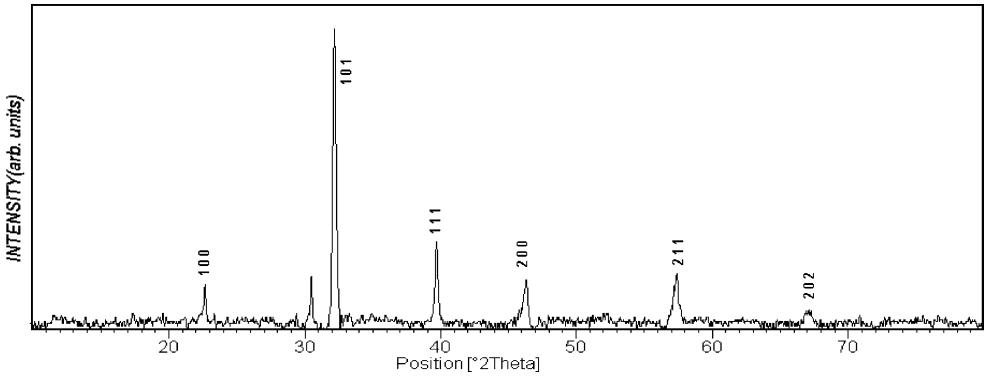

Fig. 1 X-ray diffractogram of $K_{0.5}$ $Bi_{0.5}Ti$ O_3

phase does not affect the ferroelectric character of KBT. The experimental density and X-ray density of the sample is found and given in the Table 1.

The systematic procedure for the analysis of AC measurements is to plot the results in the complex impedance plane, Z′ Vs Z″. These plots are useful for determining the dominant resistance of the sample. However, these are insensitive to smaller resistances. Figure 2(a–c) plots tend to be generally semi-circle at high temperatures. All these figures show semicircles whose centers lie on axis off the real (Z′) axis by an angle θ (=απ/2), where α is the spread factor comes out to be 0.23 and from this value, the exponent n (=1−α) was found to be 0.76.It is known that at the peaks of the semicircles the equation $\omega_m\tau=1$ holds good, τ being the mean relaxation time. The peak position of the semi-circle is found to be shifting to lower frequencies with decreasing temperature. This suggests the variation of relaxation time with temperature. The relaxation is a thermally activated process. In the temperature range 30°C–300°C, Z″—Z′ complex plots are approximately linear deviating away from Z″—axis, indicating insulating nature of the sample.

The decrease of the size of the semi-circle with temperature suggests that the bulk relaxation in the sample varies with temperature in the frequency range studied. The semi circles at high frequency correspond to the bulk response of the grains of the sample as is commonly observed in other ceramics also [22–24].

Semicircles are observed above 300°C and below this temperature; the grain boundary resistances cannot be separated out, as there are no complete semi circles. The Z′ and Z″ values decrease with temperature. In the present materials, it is clear that both bulk and grain boundary impedance are present in the ceramics, and the electrical properties are determined in general by a combination of impedance from both bulk as well as grain boundary effects. Each of these components may be represented by a parallel RC element and the simplest appropriate equivalent circuit is a series array of parallel RC elements. From the impedance data it is desired that one can separate out each of the parallel RC elements and measure their R and C values. The variation of magnitudes of RC components of the equivalent circuit may arise either because of composition changes and temperature. The key point in determining RC elements depends on the formalism used and relative magnitudes of the components. Hence it is useful to plot different admittance functions for determining RC elements and their magnitudes.

The Z′ and Z″ plots at higher temperatures can be resolved into two semi circles representing two RC circuits in series. [25], the impedance diagram in high frequency regions typically corresponds to the bulk properties [22].

The intercept of first semi circle on Z′ axis of Z′ Vs Z″ plot gives bulk resistance R_b. The specific relaxation frequency f_m (peak frequency) is identified from the plot. The bulk capacitance can be calculated using $2\pi f_m R_b C_b=1$. The values are given in the Table 2.

Figure 3(a) Shows, Arhenius plot of bulk resistance for KBT sample. The activation energy is calculated from the slope of plot and it is 1.16 ±0.04 eV. Figure 3(b) shows Arhenius plot of grain boundary resistance for KBT samples. The activation energy was calculated from the slope of the plot as 1.07±0.12 eV and it is difficult to separate out R_{gb} at low temperatures

The impedance data can also analyze, by re-plotting them in the electric modulus formalism. As is well known, the complex modulus plots are useful in determining the smallest capacitances.

Table 1 Lattice parameters and density of $K_{0.5}Bi_{0.5}TiO_3$ sample.

Compound	Lattice parameters	Experimental density(gr/cm^3)	X-ray density gr/cm^3)	% density	Porosity %
$K_{0.5}Bi_{0.5}TiO_3$	a=3.93 Å, c=4.02 Å	5.65	5.93	95	5

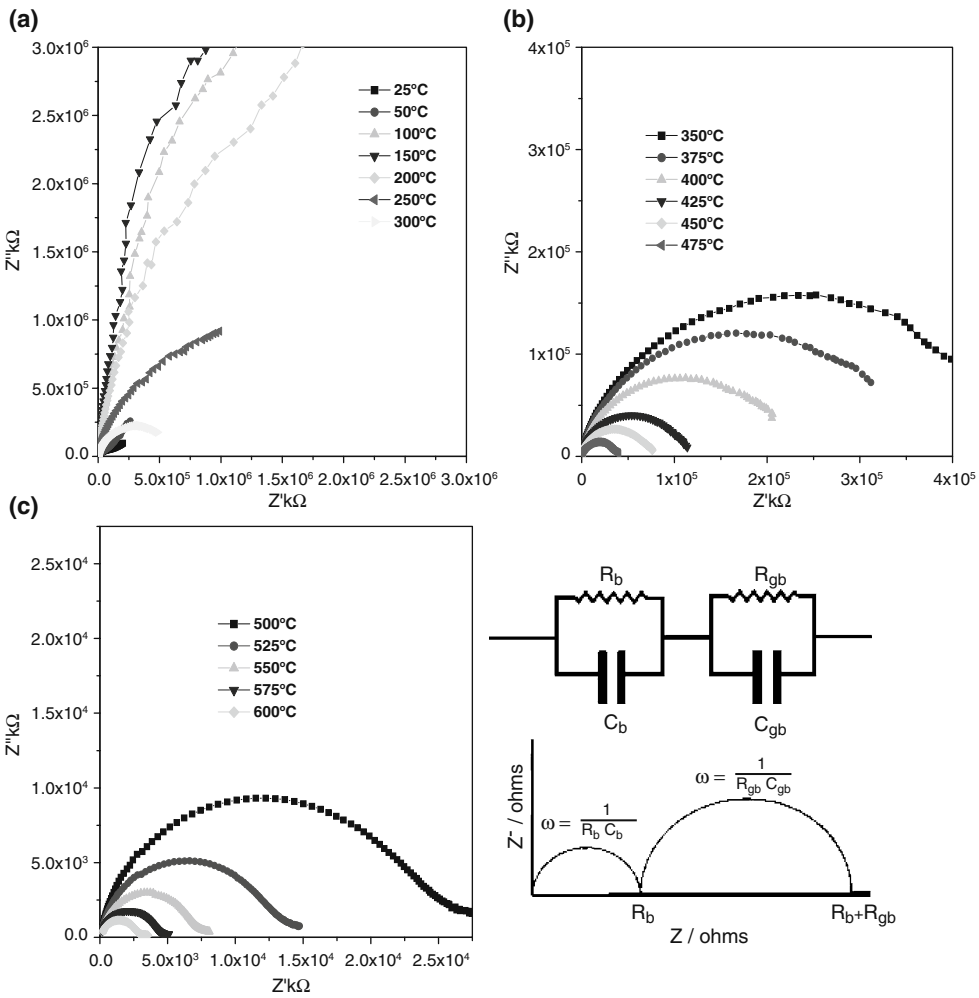

Fig. 2 (**a**–**c**), Z′ Vs Z″ at different temperatures

The relation between electric modulus and the impedance is given as

$$M' = \omega\varepsilon_0 Z''$$
$$M'' = \omega\varepsilon_0 Z'$$
$$M'' = 1/C\left(\omega\tau_m/1+\omega^2\tau_m^2\right)$$

Where τ_m is the Maxwell time constant and is equal to RC

As the ideal sample is idealized as a circuit consisting of R and C

Figure 4(a–c) presents the imaginary component of electric modulus (M″) as a function of logarithm frequency of the signal at different temperatures. In real system the peaks are broader and asymmetric. As M″ is inversely proportional to the capacitance, only bulk effects are observed as the bulk is geometric capacitance is of the order of pico farads, where as layer effects are suppressed due to their great capacitance. In all data sets, a single Debye peak in frequency on a log scale was observed. As temperature increased from the 300°C to 600°C the M″ peak is shifted to higher frequencies, while there is no much change in the height of peaks except at temperatures 575°C and 600°C. However the peak values of M" are varies from $6*10^{-4}$ to $7*10^{-4}$ in the temperature range of 300°C to 550°C. It is observed that there exist a broad peak around 1 kHz in the temperature range250°C to 400°C.

Table 2 Series resistance R_s, Bulk resistance R_b, relaxation frequency (f_o) of first semi circle, bulk capacitance (C_b), Grain boundary resistance (R_{gb}) and Grain boundary capacitance (C_{gb}) of KBT.

Temperature (°C)	R_S (Ω)	R_b (Ω)	f_o(Hz)	C_b (F)	R_{gb} (Ω)	f_{gb} (Hz)	C_{gb}(F)
600	104	2666	117700	$5.1*10^{-10}$	747	100000	$2.1367*10^{-9}$
575	180	3904	73970	$5.5*10^{-10}$	992	900000	$1.78355*10^{-10}$
550	234	6516	42290	$5.7*10^{-10}$	1448	628000	$1.7511*10^{-10}$
525	289	12217	18310	$7.1*10^{-10}$	2456	327500	$1.97971*10^{-10}$
500	541	19758	10480	$7.7*10^{-10}$	6908	141700	$1.62674*10^{-10}$

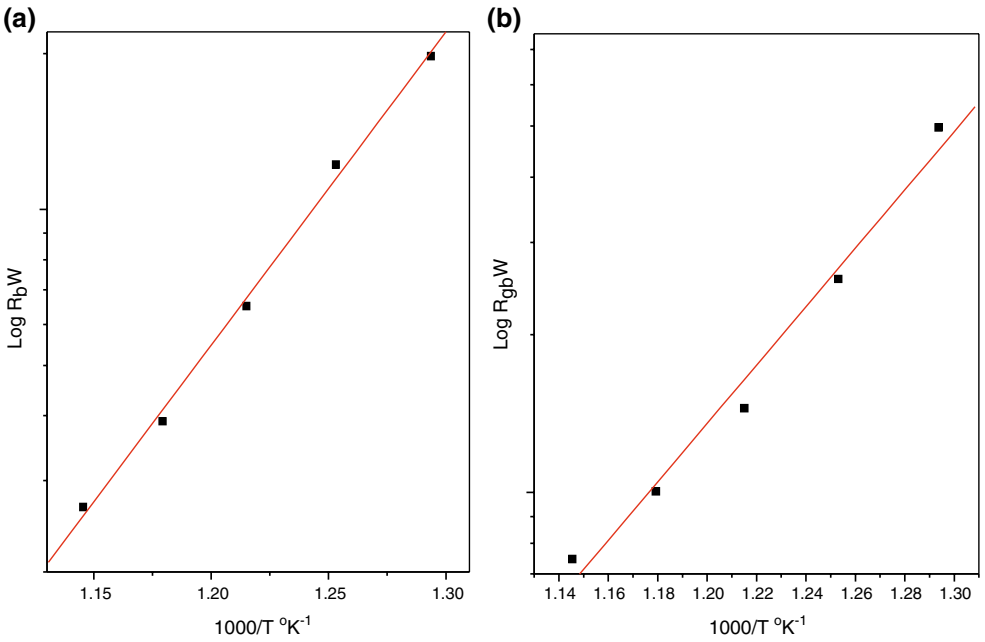

Fig. 3 Arrhenius plot of R_g and R_{gb}

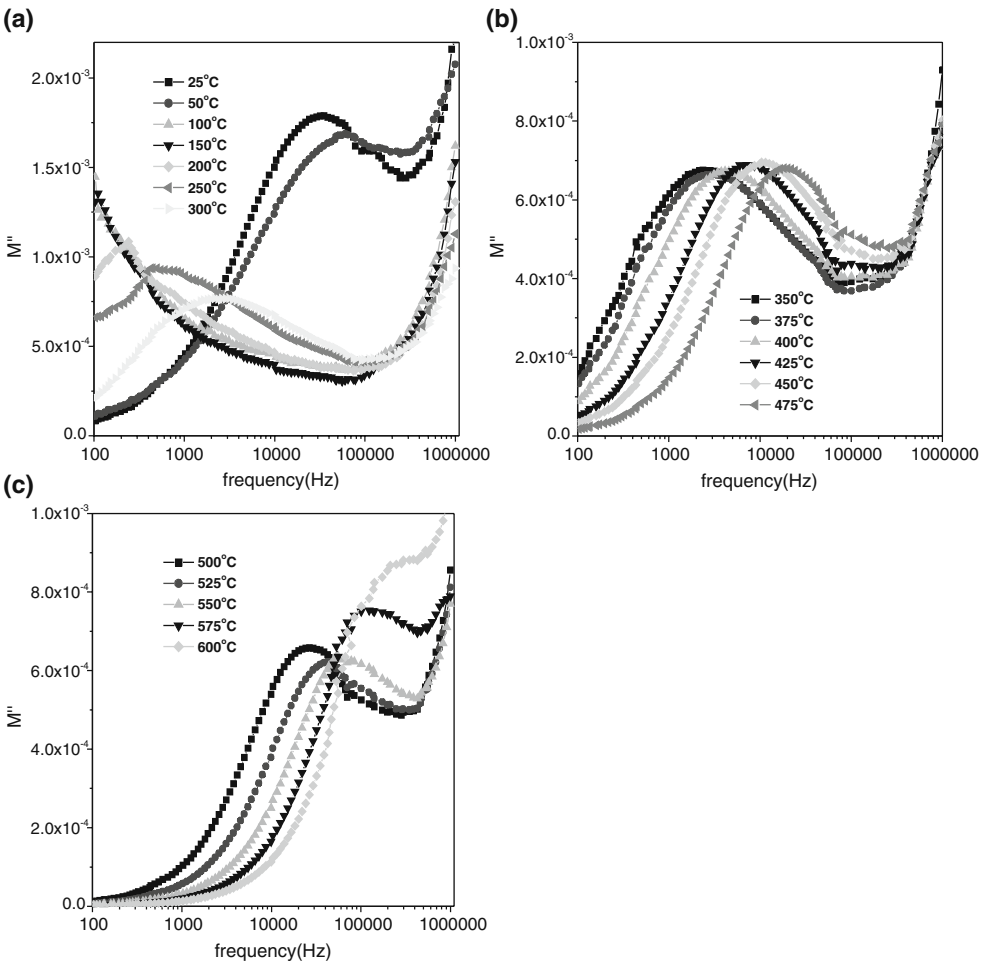

Fig. 4 (**a-c**) Variation of M″ with frequency

In the case of M″ plots, there is an apparent shift in f_{max} (at 525°C), an approximately constant peak value of M″, this would imply a variation in R but not in C. Such a non-ideal response, in the regime of temperature studied would indicate that the material cannot be represented by an equivalent circuit consisting of one single ideal RC element to model the bulk, but would have one or more parallel RC elements in series with it. According to XRD studies, in the temperature range of 380–410°C, both cubic and tetragonal phases are present simultaneously. One is polar phase while the other is a non-polar phase.

Beyond 400°C, there exists no peak in the lower frequency range selected. The peaks at lower temperatures at lower frequencies can be attributed to the grain boundaries. There is a slight change in the capacitance values as observed from the peak heights at M″ values. The variation of the capacitance can be explained on the basis of the heterogeneous grain boundaries as a result of the existence of two phases, one the polar phase and second the non-polar phase. Beyond 410°C, the cubic phase predominates as per the XRD studies. The M″ values at high frequencies in the range selected vary with temperatures.

The advantage with the electric modulus formalism is clearly seen. The relaxations, which are not seen in the impedance formalism, are seen here with temperature range 200°C–450°C. Therefore, the combination of electric modulus and impedance formalism indicates the relaxation with entire range of temperature and the frequency interval studied.

The relaxation times (τ_m) are computed from the peak frequency, using the relation $2\pi f_p\ \tau_m=1$, where f_p is the peak frequency obtained from the frequency explicit plots of M″.

Figure 5 shows the variation of relaxation time (log τ_m) versus 1000/T. The nature of variation is almost linear over a wider temperature region obeys the Arrhenius relationship:

$$\tau_m = \tau_0 e^{-E/kT},$$

Where k is boltzman constant,

There is a change of slope around 485°C .The slope change indicate the activation energy values of 0.56± 0.03 eV and 1.08±0.05 eV above and below 485°C.The higher activation energies below 485°C indicate that dipole relaxation in the presence of a polarizing field and hence require more energy.

The dielectric constant values can also be computed from the impedance data. Such data computation gives an unambiguous permittivity and transition temperature values. The impedance measurements are done with out electric poling and dielectric constant can be evaluated from the actual grain of the samples avoiding the grain boundary effects. The grain boundary effects may be positive or negative in dielectric constant of samples. The

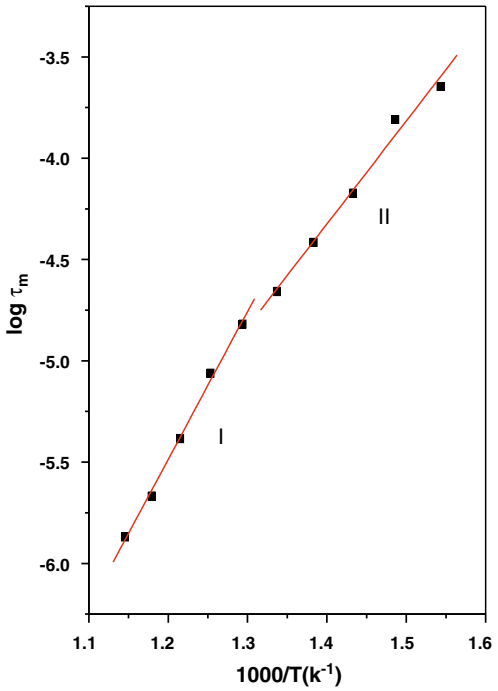

Fig. 5 Variation of relaxation time with temperature

electric poling some times gives raise defect creation, micro cracks or a change in the nature of the sample. Therefore, the evaluation of permittivity value is supposed to be more reliable.

The electrical data measured as Z* is used to calculate the relative permittivity ε'_r, at the frequencies 100 KHz, 500 KHz and 1 MHz, using the relation

$$\varepsilon'_r = \frac{Z''}{j\omega C_O |Z|^2}$$

Where, C_O is the free air capacitance [26].

The variation of dielectric constant and loss as computed from impedance measurements, as a function of temperature and frequency is shown in the Fig. 6(a, b). The dielectric curves appeared to be different from those obtained in the poled samples. It is rather puzzling whether the true structural transition is depicted here. Now in the present case there appears a hump around 350°C with frequency dependence, there after the dielectric constant peaks around 550°C. Upon increasing the field frequency from 100 Hz–1 MHz, the dielectric constant decreases as is normal in this sort of ferroelectrics.

The above result has to be viewed from the observation of Isupov et al. (2005) [1]. According to them, a structural phase transition from tetragonal cubic (higher symmetry phase) occurs around 540°C. It should also be noted here that a hump in the dielectric plot observed in the samples around 540°C. Therefore, the region between 350–540°C may not be totally in the ferroelectric phase. Even though,

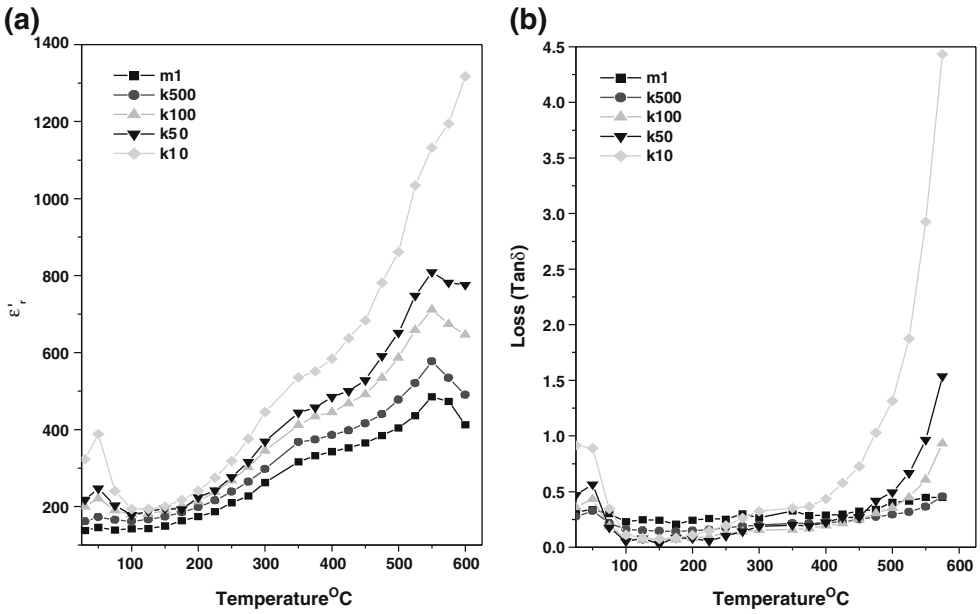

Fig. 6 (**a**, **b**) Variation of dielectric constant and loss with temperature

the ferroelectric phase is present below 400°C in this particular compound, probably, the ferroelectric transition is normally suppressed by structural phase transition. The diffusive nature of the dielectric behavior between 380–440°C may be due to ferroelectric non-polar phases in the sample. Such non-polar phases may create regions in the grains that may lead to diffusiveness of the transition. The loss values are low in the sample (Fig. 4(b),

The Arrhenius plot of DC conductivity of KBT sample has shown in Fig. 7. The room temperature resistivity of the sample is $5.2*10^8$ Ω.cm. The resistivity of the sample has not changed by impurity phase. From the graph, the activation energies have been determined in two temperature regions using the relation:

$$\sigma = \sigma_0 e^{-E/kT},$$

Where, E is the activation energy.

The value of E is of 0.54±0.03 eV below 440°C, is about 0.850±0.013 eV in the temperature range, 440°C to 575°C.

The electrical conductivity studies of an electro ceramic are complex. The real part of the conductivity (σ) is called the polarization conductivity and is a function of frequency and temperature. It is known to follow the power law proposed by Jonscher [27]

$$\text{As } \sigma_T(\omega) = \sigma(0) + A\omega^n,$$

Where σ_T is the total conductivity, σ (0) is the frequency independent conductivity, and the ac coefficient A and the power exponent n are temperature and material dependent [27].

The ac conductivity σ′ is obtained from the real part of impedance as

$$\sigma'_{ac}(\omega) = y'*t/A$$

Where, t/A is the geometrical factor of the sample, t is thickness and A is area of the sample.

The log σ'_{ac} is plotted against 10^3/T at varies frequencies shown in the Fig. 6. It should be mentioned here that even the log σ'_{ac} Vs 10^3/T also shows anomaly with slopes around the transition temperature.

It is clear from the figure that the conductivity is a function of frequency and temperature. As one observes from the frequency dependent values there are four distinct

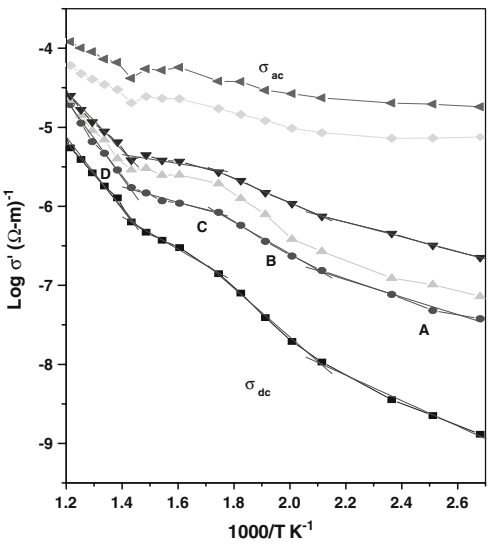

Fig. 7 Arrhenius plot of DC and AC conductivity

Table 3 Depiction of the temperature regions and associated activation energies for KBT ceramics.

KBT	100–200°C(A)	200–300°C(B)	300–425°C(C)	425–600°C(D)
DC Conductivity	0.34±0.11	0.62±0.12	0.41±0.09	0.92±0.28
10 kHz	0.22±0.11	0.40±0.07	0.20±0.11	0.97±0.18
100 kHz	0.19±0.02	0.30±0.03	0.12±0.18	0.73±0.15

temperature regions in each plot. For example the plot at 10 kHz has four distinct regions as in the case of conductivity plots for 100 kHz and DC. The activation energies associated in the four regions given in the Table 3.

As frequency increases, the activation energies are found to decrease in all regions. The plots appear to flatten at higher frequencies and exhibit a temperature independent behavior .The 'knees that are appear one region to other region are found to be 200°C, 305°C, 425°C. The sample appears to go into the intrinsic region from the DC conductivity point of view.

From the angle of the polarization conductivity (σ′) such intrinsic behavior is not clear. Probably the intrinsic region from conductivity is above 580°C. The candidate has not attempted to go into the temperature regions above 600°C in view of the experimental difficulties.

The flattening of the conductivity plots with frequency appears to result from the multiple relaxations [28]. The multiple relaxations are possible as the dipoles have different possible orientations and the dipoles by nature slightly differ from each other.

The grain boundaries are dominant almost up to 300°C and also contribute to the conduction mechanism. The defect ion complexes tend to dissociate. The activation energy above 300°C region may be the migration energy for the charges. The above studies do not exactly pin point the charge species that are involved in the conduction. They can be the A- site vacancies like potassium vacancies. The potassium ions are known to have appreciable mobility in the system in which potassium is present. The migration energy is obtained in the present studies is more or less close to the migration energy of potassium ion in the temperature range above 300°C. Potassium ion vacancies may preferably be formed over bismuth ion vacancies as bismuth ions have a large in size and mass, and tend to be immobile, If at all, the bismuth ion has to participate, it will be in the location where bismuth can go from +3 states to +4 states or vice versa. That is the electrical conductivity of bismuth oxide based ceramic crystals is attributed to a mechanism of small polar-on hopping between the occupied to unoccupied valency states [29, 30].

The hopping conduction in localized state gives rise to frequency dependent ac conductivity of ceramics. The ac conductivity of the sample depends on the dielectric nature of the sample. The conductivity arises as a result of charge hopping from one site to another site. This is evident by A.C. conductivity plots given in the Fig. 8(a–d). The Ti^{3+}–V_O'' complexes and other defects may form and inhibit the conductivity. The polarization field present in the sample below 400°C may also inhibit the conductivity.

The other vacancy species can be the oxygen vacancies. The material is sintered at high temperature and may cause the oxygen to escape. But during subsequent cooling, the oxygen reenters into the crystal. Normally it may not completely compensate the oxygen loss. This may results in oxygen vacancies apart from the vacancies created from the thermodynamic reasons. However, the activation energy values are found in the region between 325–400°C less than the value of activation energy (1 eV) for oxygen vacancy, indicating that possibly that the oxygen vacancy migration may not be a major participant for conduction mechanism [28]. Above 400°C the crystal cannot have a simple conduction mechanism like hopping mechanism. In any crystal containing ionic bonding, ionic conductivity is expected to be there. Therefore a crystal like KBT should show mixed conduction. Mixed conduction is because of hopping at the ionic migration through vacancies. Both oxygen as well as potassium vacancies.

Figure 7 shows the ferroelectric hysteresis loop of KBT at room temperature. The figure depicts the coercive field

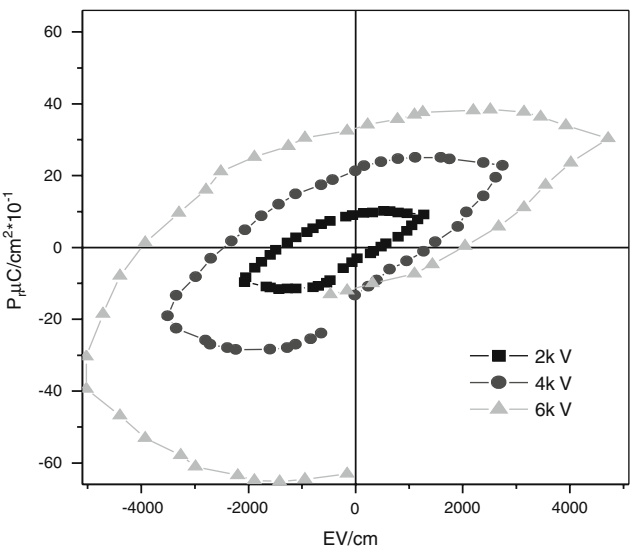

Fig. 8 Hysteresis loop at room temperature

E_C and remnant polarization P_r. It is observed that the loop area is increased as the applied voltage has increased. The remnant polarization P_r and coercive field E_C are also increased as the applied voltage is increased. The ferroelectric loop indicates the KBT sample has high loss in energy. Although there is a rounded loop might be caused by the leakage current at high voltage position (6 kV); the results indicate that the small $K_4Ti_3O_8$ (JCPDS file NO.41-0167 discussed in X-ray diffraction data) impurity presence does not affect the ferroelectric character of KBT. The obtained values of P_r and $E_{C\ to}$ be 2.13 μC/cm^2 and 1.3 kV/cm at an applied voltage of 2 kV.When compared with NBT sample, the values are less. (For NBT, P_r=38 μC/cm^2 and E_C=73 kV/cm).

Suchanicz et al. [31] reported the temperature dependence of the remanant polarization obtained from Pyroelectric measurements at 0and 100-bar pressure. Their results show that KBT has relatively high remanant polarization about 49 μC/cm^2 at room temperature, which remains non zero up to 435°C.

The d_{33} value has been measured for the poled KBT sample. The poling of piezoelectric ceramics after fabrication is an important stage in the results obtained for the samples. Because of the possibility of dielectric break down under high-applied fields, the objective in all poling situations is to induce the maximum degree of domain re-orientation for the lowest applied field and in the shortest possible time. Poling treatment carried out in the temperature range from room temperature to 150°C and in the electrical field range from 3–5 kV/mm. The piezoelectric constant d_{33} obtained is 57pC/N. Hiruma et al., observed the maximum of k_{33} (0.34) at 150°C and the piezoelectric constant d_{33} (69.8pC/N) on Hot pressed KBT (1080°C) [19].

4 Conclusions

KBT ceramics were prepared by solid-state double sintering method. Lattice parameters reveal the tetragonal structure at room temperature. Cole- Cole plots were analyzed for grain and grain boundary resistance. Dielectric maximum was observed at 380°C. Ferroelectric nature was determined using the hysteresis measurements. A.C and DC conductivity was measured and relaxation times were calculated. The d_{33} value observed as 57pC/N.

Acknowledgements We acknowledge the helpful discussions of Prof. S.V. Suryanarayana and one of the authors (PVB) acknowledges Principal & management, CVR College of Engg, for encouragement and support.

References

1. V.A. Isupov, Ferroelectrics **315**, 123 (2005)
2. J. East, D.C. Sinclair, J. Mater. Sci. Let **16**, 422 (1997)
3. J. Suchanicz, Mater. Sci. Eng. B **55**, 114 (1998)
4. T. Takenaka, K. Sakata, K. Toda, Ferroelectrics **106**, 375 (1990)
5. J. Suchanicz, J. Kwapulinski, Ferroelectrics **165**, 249 (1995)
6. J. Suchanicz, Ferrolectrics **200**, 319 (1997)
7. B.V. Bahugunab Saradhi, K. Srinivas, G. Prasad, S.V. Bhima Suryanarayana, T. Sankaram, Mater. Sci. Eng. B. **98**, 10 (2003)
8. S.B. Vakrusheb, V.A. Isupov, B.E. Kvyakovsky, N.M. Okineva, I.P. Pronon, G.A. Smolenskii, P.P. Syrnikov, Ferroelectrics **63**, 153 (1985)
9. S. Kuharuangrong, J. Mater. Sci. **36**, 1727 (2001)
10. Y. Hosono, K. Harada, Y. Yamashtta, Jpn. J. Appl. **40**, 5722 (2001)
11. G.A. Smolenskii, Sov. Phys. Solid State. **1**, 1562 (1959)
12. V.V. Ivanova, A.G. Kapyshev, Yu. N. Venevtsev, G.S. Zhdanov, Izv. AN SSSR, Ser. fiz. **26**(3), 354 (1962)
13. M.S. Gadzhiyev, A.K. Abiyev, V.A. Isupov, I.H. Ismailzade, Fiz. Tverd. Tela **27**(8), 2507 (1985)
14. Z.F. Li, C.L. Wang, W.L. Zhong, J.C. Li, M.L. Zhao, J. Appl. Phys. **94**, 2548 (2003)
15. T. Zaremba, J. Therm. Anal. Cal. **74** (2003)
16. S.M. Emel'yanov, I.P. Rayevskii, O.I. Prokopalo, Fiz.Tverd.Tela **25**(5), 1542 (1983)
17. S.M. Emel'yanov, Fiz.Tverd.Tela **28**(8), 2511 (1987)
18. C.H. Yang, Zh Wang, H.Y. Xu, Zh H. Sun, F.Y. Jiang, J.P. Zh, J.R. Han, J. Cryst. Growth **262**, 304 (2004)
19. Y. Hiruma, R. Aoyagi, H. Nagata, T. Takenaka Jpn. J. Appl. Phys. **44**(7A), (2005)
20. R.L. Byer, C.B. Roundy, Ferroelectrics **3**, 333 (1972)
21. B. Jaffe, W.R. Cook, H. Jaffe, *Piezoelectric ceramics* (Academic, London, 1971), p. 288
22. D.C. Sinclair, J. East, J. Appl. Phys. **66**, 3580 (1989)
23. B.V. Bahuguna Saradhi, K. Srinivas, G. Prasad, S.V. Suryanarayana, T. Bhimasankaram, Mat. Sci & Engg. B **98**, 10 (2003)
24. A.P. Barranco, M.P.G. Amador, A. Huanosta, R. Valensuela, J. Appl. Phys. Lett. **73**, 2039 (1998)
25. K.S. Cole, R.H. Cole, J. Chem.Phys **9**, 341 (1941)
26. I.M. Hodge, M.D. Ingram, A.R. West, J. Electro Anal. Chem **74**, 125 (1976)
27. A.K. Jonscher, J.Mater.Sci **16**, 2037 (1981)
28. B.V. Bahuguna Saradhi, K. Srinivas, G. Prasad, S.V. Suryanarayana, T. Bhimasankaram, Int. J. Mod. Phy. B **16**, 4175 (2002)
29. T. Takenaka, K. Sakata, Sensor Mater **1**, 123 (1988). (1984) 205
30. C. Moure, L. Lascano, J. Tartaj, P. Duran, Ceramics International **29**, 91 (2003)
31. J. Suchanicz, K. Roleder, A. Kania, J. Handerek, Ferroelectrics **77**, 107 (1988)